

The Astrophysical Consequences of Intervening Galaxy Gas on Fast Radio Bursts

J. Xavier Prochaska,¹★ Marcel Neeleman,¹

¹*Astronomy & Astrophysics, UC Santa Cruz, 1156 High St., Santa Cruz, CA 95064 USA*

Accepted XXX. Received YYY; in original form ZZZ

ABSTRACT

We adopt and analyze results on the incidence and physical properties of damped Ly α systems (DLAs) to predict the astrophysical impact of gas in galaxies on observations of Fast Radio Bursts (FRBs). Three DLA measures form the basis of this analysis: (i) the HI column density distribution, parameterized as a double power-law; (ii) the incidence of DLAs with redshift (derived here), $\ell_{\text{DLA}}(z) = A + B \arctan(z - C)$ with $A = 0.236^{+0.016}_{-0.021}$, $B = 0.168^{+0.010}_{-0.017}$, $C = 2.87^{+0.17}_{-0.13}$; and (iii) the electron density, parameterized as a log-normal deviate with mean $10^{-2.6} \text{ cm}^{-3}$ and dispersion 0.3 dex. Synthesizing these results, we estimate that the average rest-frame dispersion measure from the neutral medium of a single, intersecting galaxy is $\text{DM}_{\text{DLA}}^{\text{NM}} = 0.25 \text{ pc cm}^{-3}$. Analysis of AlIII and CII* absorption limits the putative warm ionized medium to contribute $\text{DM}_{\text{DLA}}^{\text{WIM}} < 20 \text{ pc cm}^{-3}$. Given the low incidence of DLAs, we find that a population of FRBs at $z = 2$ will incur $\overline{\text{DM}}_{\text{DLA}}^{\text{NM}}(z_{\text{FRB}} = 2) = 0.01 \text{ pc cm}^{-3}$ on average, with a 99% c.l. upper bound of 0.22 pc cm^{-3} . Assuming that turbulence of the ISM in external galaxies is qualitatively similar to our Galaxy, we estimate that the angular broadening of an FRB by intersecting galaxies is negligible ($\theta_{\text{scatt}} < 0.1 \text{ mas}$). The temporal broadening is also predicted to be small, $\tau_{\text{DLA}} \approx 0.3 \text{ ms}$ for a $z = 1$ galaxy intersecting a $z = 2$ FRB for an observing frequency of $\nu = 1 \text{ GHz}$. Even with $\nu = 600 \text{ MHz}$, the fraction of sightlines broadened beyond 25 ms is only approximately 0.1%. We conclude that gas within the ISM of intervening galaxies has a minor effect on the detection of FRBs and their resultant DM distributions. Download the repository at <https://github.com/FRBs/FRB> to repeat and extend the calculations presented here.

Key words: (galaxies:) intergalactic medium – galaxies: ISM

1 INTRODUCTION

The discovery of the ‘repeating’ Fast Radio Burst (Spitler et al. 2016, FRB) and subsequent follow-up observations at the Very Large Array (Chatterjee et al. 2017) have led to the confirmation that at least some FRB events have an extragalactic origin (Tendulkar et al. 2017). In turn, the large Dispersion Measure (DM) that essentially defines an FRB offers one the opportunity to study the integrated electron column density along individual sightlines through the universe. New and upcoming surveys – e.g. CHIME (Bandura et al. 2014), ASKAP (Bannister et al. 2017), APERTIF, REALFAST (Bower et al. 2016) – will yield a terrific set of observations to measure baryons in the $z < 1$ universe and possibly beyond, complementing decades of work in the far-UV (e.g. Davé & Tripp 2001; Chen et al. 2005; Tejos et al. 2014).

For a source at great distance, e.g. $z \sim 1$ or approximately 2.4 Gpc, one expects a significant DM from the diffuse, highly-ionized intergalactic medium (Inoue 2004, IGM;). In quasar absorption line (QAL) parlance, this plasma is referred to as the Ly α forest. Gas in the dark matter halos of galaxies will also contribute and may even dominate (McQuinn 2014, ; Prochaska & Zheng 2017, in prep.). This gas in QAL research is referred to as the circumgalactic medium (CGM), which one frequently associates to the optically thick Lyman limit systems (LLSs; e.g. Fumagalli et al. 2011; Ribaldo et al. 2011; Hafen et al. 2016). Most rarely, an FRB sightline may penetrate the ISM of a galaxy akin to our own. If the neutral hydrogen column density N_{HI} equals or exceeds $2 \times 10^{20} \text{ cm}^{-2}$, the QAL community refers to the absorption as a damped Ly α (DLA) system (Wolfe et al. 1986, 2005). In the far-UV, a DLA system shows a quantum mechanically ‘damped’ Ly α line with equivalent width $W_{\text{Ly}\alpha} > 10 \text{ \AA}$. In addition to contributing to the DM value of an FRB, the free electrons in DLAs – if turbulent – will

★ E-mail: xavier@ucolick.org

scatter the radio pulse (Macquart & Koay 2013). Turbulent scattering broadens both the angular size of the source and the intrinsic duration of the event.

The DLA contribution to DM is distinct from other intervening gas because: (1) DLAs arise in collapsed (i.e. highly non-linear) structures; and (2) they trace a predominantly neutral gas with ionization fraction $x \equiv n_{\text{H}^+}/n_{\text{H}} \ll 1$. We emphasize that the analysis performed here considers primarily the neutral gas of DLAs, i.e. the warm and cold neutral media (WNM/CNM) of external galaxies. We also consider a putative warm ionized medium (WIM) surrounding DLAs. We explicitly ignore, however, gas in the dark matter halos hosting DLAs which is believed to be traced by high ions like C^{+3} and Si^{+3} (Wolfe & Prochaska 2000a,b; Maller et al. 2003; Fox et al. 2007; Prochaska et al. 2008a). The astrophysical impact of galactic halos on FRBs will be treated in a companion paper (Prochaska & Zheng 2017, in prep.; see also McQuinn 2014).

We recognize that the DLA criterion is somewhat arbitrary and gas with modestly lower column densities (the so-called super Lyman limit systems or sub-DLAs) may be qualitatively similar and may also arise in the ISM of intervening galaxies. However, most of these systems trace gas in the halos of galaxies and therefore we will examine such systems explicitly in the companion paper. We note that the code provided with this paper can easily be modified to include such material within the framework developed here.

It has been proposed that intervening galaxies will essentially ‘extinguish’ the FRB signal by broadening the pulse duration to a non-detectable signal (Macquart & Koay 2013; McQuinn 2014). Analogous to dust obscuring UV-bright quasars to bias observed sightlines against a subset of DLAs (Ostriker & Heisler 1984; Fall & Pei 1993), it is possible that the observed FRB population will not occur along sightlines that intersect galaxies. In turn, this may bias the observed DM distribution and alter the observed redshift distribution of FRBs. A precise characterization of these effects is therefore critical to inferring the intrinsic nature of FRBs and for utilizing the population to constrain cosmological quantities (e.g. Gaensler et al. 2008).

In this paper, we analyze the latest results from DLA surveys to empirically estimate the impact of DLAs on current and future FRB studies. This includes statistics on the incidence of DLA absorption $\ell_{\text{DLA}}(z)$, the frequency distribution of N_{HI} , aka $f(N_{\text{HI}}, z)$, and constraints on the electron volume density n_e . Throughout, we adopt the Planck 2015 cosmology (Planck Collaboration et al. 2016) encoded in *astropy* (v1.3). All of the calculations presented here may be reproduced and extended using codes in this repository: <https://github.com/FRBs/FRB>.

2 THE DISPERSION MEASURE OF DLAS

As emphasized above, gas in intervening galaxies will contribute to the DM of FRBs for those sightlines that intersect any such galaxies. On the reasonable ansatz that *all* galaxies with a non-negligible DM will also have an N_{HI} value satisfying the DLA criterion, we may use statistics and measured properties of the latter to predict the effects of the former. This forms the basis of our methodology.

We may construct an empirical estimate for the average

DM value from the neutral medium in DLAs for a FRB at redshift z_{FRB} , $\overline{DM}_{\text{DLA}}^{\text{NM}}(z_{\text{FRB}})$, as follows. Formally, we have,

$$\overline{DM}_{\text{DLA}}^{\text{NM}}(z_{\text{FRB}}) = \int_0^{z_{\text{FRB}}} \int_{10^{20.3}}^{\infty} f(N_{\text{HI}}, z) N_{\text{HI}} x_{\text{DLA}}(N_{\text{HI}})(1+z)^{-1} dN_{\text{HI}} dz \quad , \quad (1)$$

where we have defined $x_{\text{DLA}} \equiv n_e/n_{\text{H}}$ with $n_{\text{H}} \approx n_{\text{HI}}$ for the predominantly neutral DLAs. One recognizes $f(N_{\text{HI}}, z)$ as the H I frequency distribution, i.e. $f(N_{\text{HI}}, z) dN_{\text{HI}} dz$ is the estimated number of DLAs in N_{HI} and redshift intervals.

Thus far, DLA surveys have not revealed a significant evolution in the shape of $f(N_{\text{HI}}, z)$ with redshift¹. Therefore, we will assume that the function describing $f(N_{\text{HI}}, z)$ is separable (see also Inoue et al. 2014), i.e.

$$f(N_{\text{HI}}, z) = h(N_{\text{HI}}) j(z) \quad . \quad (2)$$

For the first term, we adopt the double power-law derived by Prochaska et al. (2005) from their analysis of the SDSS-DR5:

$$h(N_{\text{HI}}) = K \left(\frac{N}{N_d} \right)^{\beta} \quad \text{where } \beta = \begin{cases} \alpha_3 : N < N_d; \\ \alpha_4 : N \geq N_d \end{cases} \quad (3)$$

with $N_d = 10^{21.551} \text{ cm}^{-2}$, $\alpha_3 = -2.055$, and $\alpha_4 = -6$. While there have been more recent and larger surveys of DLAs from BOSS (e.g. Noterdaeme et al. 2012; Bird et al. 2017), most have not provided functional fits to their $f(N_{\text{HI}}, z)$ analysis². Furthermore, our own efforts with deep-learning techniques raises concerns on several of the reported results Parks et al. (2017). In any case, as progress on DLA surveys continues, we will ingest and update the accompanying repository³ and the results on FRBs are relatively insensitive to the precise form of $h(N_{\text{HI}})$.

To constrain $j(z)$, we perform a new calculation of the incidence of DLAs:

$$\ell_{\text{DLA}}(z) = \int_{10^{20.3}}^{\infty} f(N_{\text{HI}}, z) dN_{\text{HI}} = j(z) \int_{10^{20.3}}^{\infty} h(N_{\text{HI}}) dN_{\text{HI}} \quad . \quad (4)$$

In the following, we set the normalization K of $h(N_{\text{HI}})$ such that $\ell_{\text{DLA}}(z) = j(z)$, i.e. the integral over $h(N_{\text{HI}})$ is unity. Many DLA surveys have been analyzed to assess $\ell_{\text{DLA}}(z)$ across cosmic time (e.g. Wolfe et al. 1995; Storrie-Lombardi & Wolfe 2000; Prochaska et al. 2005; Rao et al. 2017). The standard approach is to first evaluate the search path for DLAs, a.k.a. $g(z)$ or the number of independent quasar sightlines surveyed for DLA absorption at a given redshift. A good estimator for the incidence in a finite redshift interval Δz at redshift z is

$$\ell_{\text{DLA}}(z) = N_{\text{DLA}}/\Sigma g(z) \quad (5)$$

¹ Note that this differs from the full population of QALs, e.g. Worseck & Prochaska (2011).

² An analysis of the complete SDSS survey yields $f(N_{\text{HI}}, z)$ with a fully consistent shape as the one adopted here (Noterdaeme et al. 2009).

³ <https://github.com/FRBs/FRB>

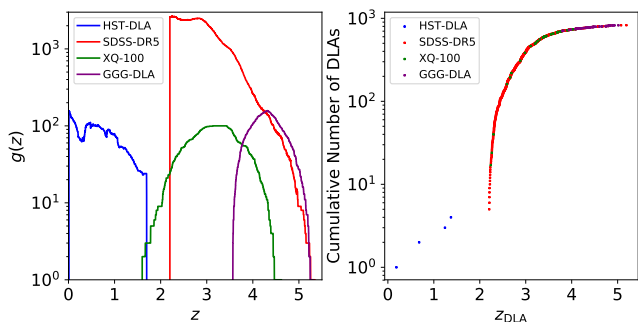


Figure 1. (left) The curves describe the survey path $g(z)$ for the datasets used to estimate the DLA incidence with redshift. The $g(z)$ curves indicate the number of quasars searched for DLAs at a given redshift. (right) The cumulative number of DLAs identified in these surveys, ranked by redshift. Note the scarcity of DLAs at $z < 2$ indicating a low incidence.

with N_{DLA} the number of DLAs detected in Δz , and the sum on $g(z)$ is performed over the same interval.

The left panel of Figure 1 summarizes the redshift path analyzed by the DLA surveys adopted here: a blind search for DLAs at $z < 2$ in Hubble Space Telescope UV spectroscopy, HST-DLA (Neeleman et al. 2016); a survey of quasars from the SDSS data release 5, SDSS-DR5 (Prochaska & Wolfe 2009); a survey of 100 quasars at $z = 3-4$ observed with the X-Shooter spectrograph, XQ-100 (López et al. 2016; Sánchez-Ramírez et al. 2016); a survey for $z > 3.5$ DLAs using the Gemini GMOS spectrometers, GGG-DLA (Worseck et al. 2014; Crighton et al. 2015). The cumulative distribution of DLAs detected, N_{DLA} , is shown in the right panel. One point is obvious from the figure: despite the survey of many hundreds of quasars at $z < 1$ with *HST*, only a handful of DLAs were detected⁴. This primarily follows from cosmological expansion, i.e. one predicts that the observed incidence decreases as $(1+z)^2$ for an unevolving population of absorbers per comoving volume in a Λ -dominated universe.

From the data in Figure 1, we have used the estimator in Equation 5 to calculate $\ell_{\text{DLA}}(z)$ in select bins (Figure 2). Here we derive uncertainties assuming Poisson statistics. It is apparent that $\ell_{\text{DLA}}(z)$ increases with redshift from low values at $z < 1$. The figure also shows an estimate for $\ell(z)$ at $z \approx 0$ based on 21 cm observations where we have combined the values reported by Zwaan et al. (2005) and Braun (2012): $\ell(z)_{21\text{ cm}} = 0.035 \pm 0.01$.

Most previous analyses of $\ell_{\text{DLA}}(z)$ have assumed it follows the functional form $(1+z)^\gamma$. This is physically motivated by cosmological expansion, but Prochaska et al. (2008b) emphasized that the evolution in $\ell_{\text{DLA}}(z)$ at $z \approx 2-3$ is not well described by such a power-law. Lacking a proper physical model for $\ell_{\text{DLA}}(z)$, we take an empirically driven approach and seek a functional form that describes the data well at all

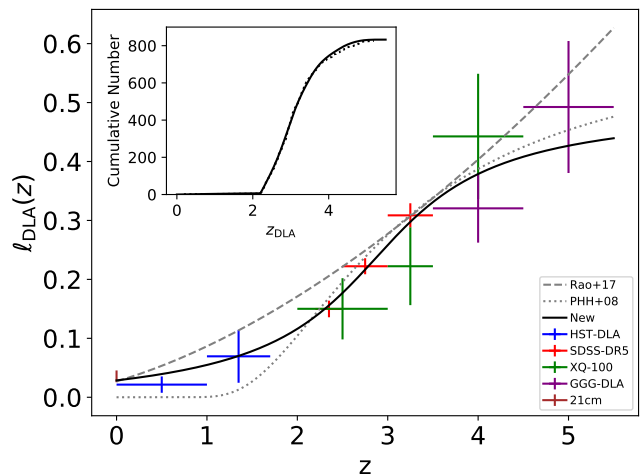


Figure 2. Incidence of DLAs per unit redshift $\ell_{\text{DLA}}(z)$ estimated from the surveys described by Figure 1. Overlaid on the binned evaluations (the x bars show bin size and the y bars indicate Poisson uncertainty) are previous fits from the literature (grey curves; Prochaska et al. 2008b; Rao et al. 2017) and our new derivation (black curve). The inset compares the observed cumulative number of DLAs to the model, and a one-sided Kolmogorov-Smirnov test yields an acceptable probability for the null hypothesis.

redshifts and with the fewest number of parameters. After some experimentation, we settled on a model,

$$\ell_{\text{DLA}}(z) = A + B \arctan(z - C) \quad (6)$$

which captures an apparent inflection in $\ell_{\text{DLA}}(z)$ at the highest redshifts studied (Crighton et al. 2015). We performed a standard maximum likelihood analysis to find the best values for A , B and C as shown in Figure 2 and listed in Table 1. Errors on these parameters were estimated using standard bootstrap techniques. All of the data and our new $\ell_{\text{DLA}}(z)$ result are ingested in the *pyigm*⁵ package.

With $\ell_{\text{DLA}}(z)$ well-fitted, we may calculate the average number of DLAs intervening a source at redshift z_{FRB} as:

$$\begin{aligned} \bar{n}_{\text{DLA}}(z_{\text{FRB}}) &= \int_0^{z_{\text{FRB}}} \ell_{\text{DLA}}(z) dz \\ &= A z_{\text{FRB}} + B [\mu \arctan \mu - \ln(\mu^2 + 1)/2 \\ &\quad - C \arctan C + \ln(C^2 + 1)/2] \end{aligned} \quad (7)$$

with $\mu \equiv C - z_{\text{FRB}}$. For a single sightline to an FRB, the uncertainty in $\bar{n}_{\text{DLA}}(z_{\text{FRB}})$ is dominated by Poisson sampling with $\sigma^2(\bar{n}_{\text{DLA}}) = \bar{n}_{\text{DLA}}$. For a population of FRBs, the uncertainty is dominated by errors in our estimation of $\ell_{\text{DLA}}(z)$. Figure 3 shows $\bar{n}_{\text{DLA}}(z_{\text{FRB}})$ versus redshift, where one recovers a value of 0.04 for $z_{\text{FRB}} = 1$ and one notes $\bar{n}_{\text{DLA}}(z_{\text{FRB}})$ remains less than unity until nearly $z_{\text{FRB}} = 5$. This relatively low incidence strictly limits the potential impact of intervening galaxies on FRBs.

⁴ We do not include here the DLA surveys of Rao & Turnshek who targeted strong Mg II absorbers to detect DLAs (Rao et al. 2006, 2017).

⁵ <https://github.com/pyigm/pyigm>

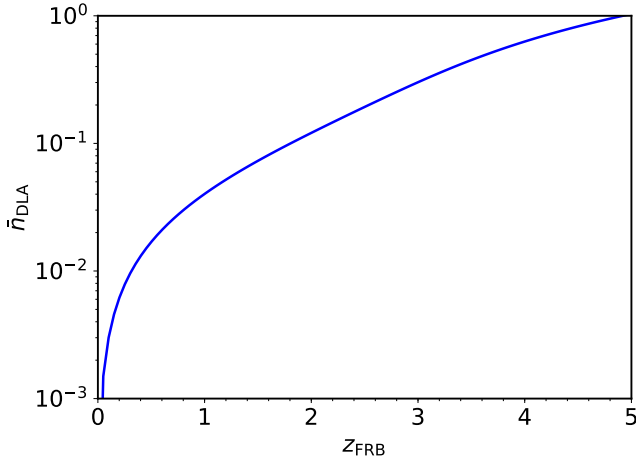


Figure 3. Average number of DLAs $\bar{n}_{\text{DLA}}(z_{\text{FRB}})$ intersected by a sightline to a source at redshift z_{FRB} . For $z_{\text{FRB}} = 1$, we estimate $\bar{n}_{\text{DLA}}(z_{\text{FRB}}) < 0.05$ and the value remains less than unity until $z_{\text{FRB}} \approx 5$. For a population of events at a given redshift, the number of DLAs observed will be Poisson distributed with mean and variance of $\bar{n}_{\text{DLA}}(z_{\text{FRB}})$. This relatively low incidence strictly limits the potential impact of intervening galaxies on FRBs.

Owing to the large HI column densities that define DLAs, the gas is (extremely) optically thick to HI ionizing radiation and one expects DLAs to be predominantly neutral gas. This has been demonstrated theoretically and empirically (e.g. Viegas 1995; Vladilo et al. 2001), although there are notable, individual counter-examples (e.g. Prochaska et al. 2002). A direct assessment of the neutral fraction of DLAs (or any QAL) is challenged by the fact that the commonly observed resonance lines are insensitive to the physical conditions of density, temperature, etc. Therefore, direct measurements of x_{DLA} are difficult to obtain.

A notable exception is to assess the physical conditions within DLAs by analyzing absorption from the excited states of C⁺ and Si⁺ (Howk et al. 2005). The most comprehensive study to date was by Neeleman et al. (2015) who used an MCMC analysis to derive estimates of the electron and hydrogen number densities n_e , n_{H} for ≈ 80 DLAs at $z \approx 2 - 5$. Figure 4 summarizes the results versus the HI column density for the 50 systems with C II* detected. There is a small trend of decreasing ionization fraction with N_{HI} that we parameterize as,

$$\log x_{\text{DLA}} = \log \frac{n_e}{n_{\text{H}}} = -2.881 - 0.352 (\log N_{\text{HI}} - 20.3) \quad (8)$$

We proceed by assuming an 0.5 dex uncertainty in n_e for any given DLA.

We now have all the ingredients necessary to offer an estimate for the average DM for a sightline intersecting one galaxy,

$$\text{DM}_{\text{DLA}}^{\text{NM}} = \frac{\int_{10^{20.3}}^{\infty} h(N_{\text{HI}}) N_{\text{HI}} x_{\text{DLA}} dN_{\text{HI}}}{\int_{10^{20.3}}^{\infty} h(N_{\text{HI}}) dN_{\text{HI}}} \approx \langle N_{\text{HI}} \rangle x_{\text{DLA}} (\langle N_{\text{HI}} \rangle) = 0.25 \text{pc cm}^{-3} \frac{\text{DM}_{\text{DLA}}^{\text{NM}}(z_{\text{FRB}}) \approx \text{DM}_{\text{DLA}} \bar{n}_{\text{DLA}}(z_{\text{FRB}}) (1 + \bar{z})^{-1}}{\quad} \quad (10)$$

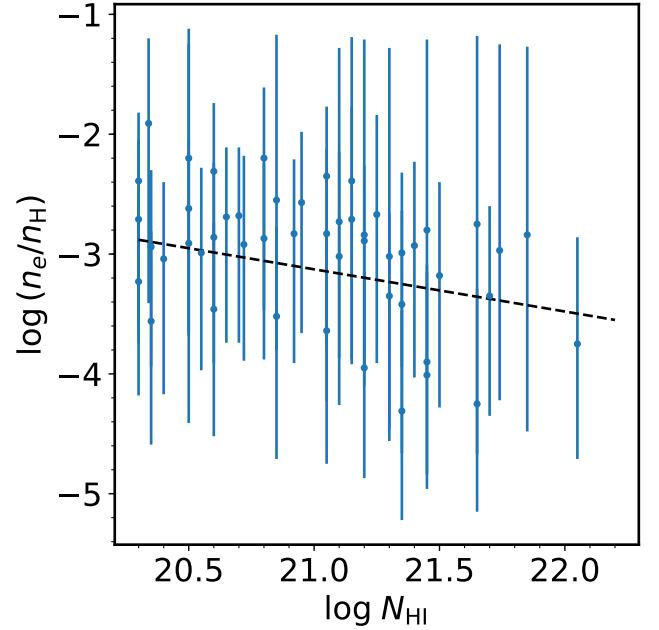


Figure 4. Estimates of the ionization fraction of DLA gas ($\log x_{\text{DLA}} = \log[n_e/n_{\text{H}}]$) from an MCMC analysis of measured column densities of ionized carbon and silicon and their associated excited levels (Neeleman et al. 2015). Overplotted on their sample is a log-linear fit, described by Equation 8.

This is substantially smaller than the lowest values measured for sightlines intersecting our own ISM (Gaensler et al. 2008, $\approx 25 \text{pc cm}^{-3}$, from the Sun).

We restrict our analysis to C II* detections because non-detections yield little constraint on the electron density. However, by restricting the n_e/n_{H} assessment to DLAs with C II* detections, we may be biased towards sightlines dominated by the CNM (Wolfe et al. 2003; Neeleman et al. 2015), and therefore lower ionization fractions. Indeed, models of a multi-phase ISM predict ionization fractions for the WNM phase of $x_{\text{WNM}} \approx 0.1$ (e.g. Wolfire et al. 1995). We note, however, that DLAs without C II* detections have systematically lower N_{HI} values. For the $\text{DM}_{\text{DLA}}^{\text{NM}}$ measurement, the ionization fraction gets weighted by N_{HI} and the bias resulting from omitting these systems is thereby at least partially offset. An additional bias toward sightlines dominated by the CNM could have been introduced from the selection criteria adopted by Neeleman et al. (2015). However, even if we assume that a majority of the gas arises in the WNM, as is indicated by 21 cm observations of radio-loud quasars with intervening DLAs (Kanevar & Chengalur 2003; Kanevar et al. 2014), the primary conclusions of the paper remain unchanged.

Because the shape of $f(N_{\text{HI}}, z)$ is taken to be invariant with redshift, the dN_{HI} integral in Equation 9 may be evaluated independently to derive an approximate expression for the average contribution for a population of FRBs at z_{FRB} :

with \bar{z} the average redshift of intervening galaxies. Evaluating Equation 10 at $z_{\text{FRB}} = 1$, we estimate $\overline{\text{DM}}_{\text{DLA}}^{\text{NM}}(z_{\text{FRB}} =$

1) $\approx 0.0065 \text{ pc cm}^{-3}$. To generate a more accurate evaluation of $\overline{DM}_{\text{DLA}}^{\text{NM}}(z_{\text{FRB}})$, we have performed a Monte Carlo simulation of 10^6 sightlines to FRBs over a series of z_{FRB} values. For each realization, we draw the number and redshifts of DLAs on the sightline according to $\ell_{\text{DLA}}(z)$, (allowing for Poisson variance in $\bar{n}_{\text{DLA}}(z_{\text{FRB}})$), assign random N_{HI} values drawn from $h(N_{\text{HI}})$, evaluate x_{DLA} , and calculate the DM value. The results are shown in Figure 5, and we find small values at all z_{FRB} . We also show the 68% and 99% intervals and find that $\sim 1\%$ of FRB sightlines originating at $z_{\text{FRB}} = 5$ will experience a contribution of $\sim 0.2 \text{ pc cm}^{-3}$ from the neutral ISM of intervening galaxies.

As emphasized above, in our Galaxy the smallest DM values measured from our position at the Sun are approximately 25 pc cm^{-3} . It is accepted that a warm ionized medium (WIM), which also generates nearly ubiquitous H α emission across the sky (e.g. Reynolds et al. 1998), is responsible for this ‘floor’ to the Galactic DM (e.g. Cordes & Lazio 2003). Several studies have used the observed DM distribution of pulsars with Galactic latitude and distance to model the density, filling factor, and distribution with scale height of electrons in the WIM (Gaensler et al. 2008; Berkhuijsen & Fletcher 2008).

The Galactic WIM is believed to be primarily generated by photons from O stars that have ‘leaked’ through their H II regions (Haffner et al. 2009). Many external galaxies at $z \sim 0$ also exhibit a WIM component typically referred to as diffuse ionized gas or DIG (e.g. Rand 1997). At high z , the presence and nature of the WIM in galaxies has not yet been established. One notes that the average star formation rate in high- z galaxies is higher which could accentuate a WIM, but the ISM may also be denser and less porous. Separately, the extragalactic UV background, which is more intense at high z , may ionize the outer ISM of galaxies to produce a WIM component.

In analogy with the Galactic ISM, it is possible that DLAs are also enveloped in layers of predominantly ionized gas, i.e. a WIM component⁶. Indeed, Howk & Sembach (1999) first emphasized that the frequent detection of Al⁺⁺ in DLAs suggests a putative warm ionized medium, noting that Al III absorption in our Galaxy traces its underlying electron distribution (Savage et al. 1990). Furthermore, the Al III absorption in DLAs more frequently traces the low-ion transitions instead of the more highly ionized gas revealed by e.g. C IV (Wolfe & Prochaska 2000a). On the other hand, one may ionize a non-negligible fraction of Al⁺ to Al⁺⁺ via hard radiation from local sources or the EUVB without significantly ionizing hydrogen because of the large cross-section of Al⁺ to high-energy photons (Sofia & Jenkins 1998; Prochaska et al. 2002). In any event, we estimate an additional contribution to DM from DLAs based on their $N(\text{Al}^{++})$ measurements. This estimate will also include any contribution from a WNM component that was not captured by our treatment above.

Specifically, we assume that Al⁺⁺ traces a predomi-

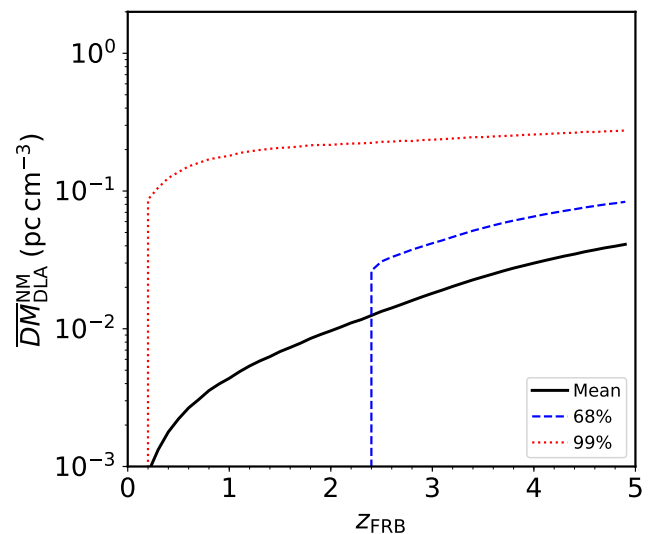


Figure 5. The solid, black curve shows the average DM due to DLAs measured from a population of FRBs at redshift z_{FRB} . For the CNM/WNM of these galaxies, we find $\overline{DM}_{\text{DLA}}^{\text{NM}}(z_{\text{FRB}}) < 10^{-1} \text{ pc cm}^{-3}$ at all $z_{\text{FRB}} < 7$. The blue-dashed and red-dotted curves show the 68% and 99% upper intervals for $\overline{DM}_{\text{DLA}}^{\text{NM}}(z_{\text{FRB}})$ calculated from 10^6 random draws. These equal zero at low z_{FRB} because of the low probability to intersect even a single galaxy (Figure 3).

nantly ionized gas ($x_{\text{DLA}} \approx 1$) and that it is the dominant ionization state of Al in this plasma. It follows that,

$$N_e \approx N(\text{Al}^{++}) - \epsilon(\text{Al}) + 12. - \log(Z/Z_{\odot}) \quad , \quad (11)$$

with $\epsilon(\text{Al})$ the number abundance of Al in the Sun (6.43; Asplund et al. 2009) and Z/Z_{\odot} the metallicity of the DLA relative to solar. Figure 6 shows DM_{AlIII} values derived with Equation 11 versus N_{HI} using the HIRES sample of Neeleman et al. (2013); statistical uncertainties of approximately 0.2 dex are dominated by the error in Z/Z_{\odot} . Even with the somewhat extreme assumptions encoded by Equation 11, we derive a median DM_{AlIII} value of less than 20 pc cm^{-3} . One also notes that the highest DM_{AlIII} values are associated primarily with high N_{HI} DLAs suggesting that this gas arises in the WNM/CNM. Altogether, we constrain $DM_{\text{DLA}}^{\text{WIM}}$ to be less than 20 pc cm^{-3} and likely less than 10 pc cm^{-3} . This upper limit is also consistent with the many non-detections of C II* absorption in DLAs (Wolfe et al. 2003).

3 SCATTERING

The radio emission from a distant, compact source that intersects a DLA may be scattered by electron density inhomogeneities in the gas. The effects include an angular broadening of the source θ_{scatt} and temporal broadening τ_{scatt} . Both exhibit a frequency dependence. The scattering processes has been studied extensively for sightlines through the ISM to pulsars in our Galaxy (Taylor & Cordes 1993), and the formalism has been developed for gas intersecting FRBs by (Macquart & Koay 2013, ; hereafter M13). We do not repeat

⁶ Note again that we distinguish here from gas in the dark matter halo presumed to contain DLAs. This CGM component is discussed in a separate manuscript (Prochaska & Zheng 2017, in prep.; see also McQuinn 2014).

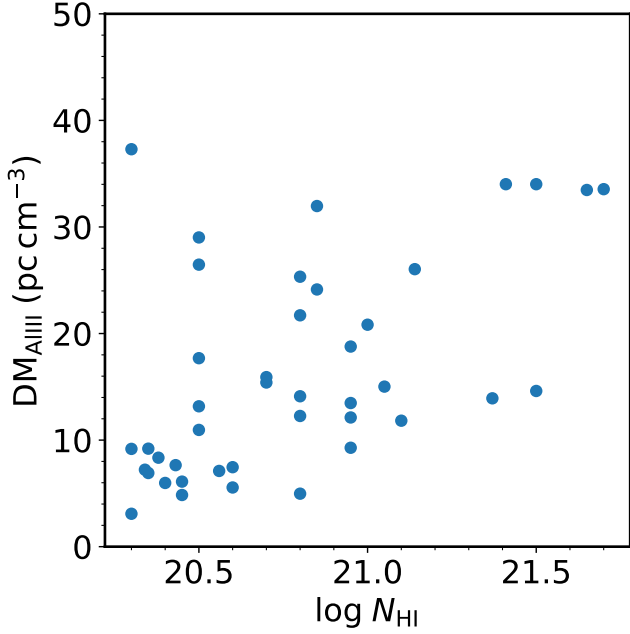


Figure 6. The points track estimates of DM for a putative WIM component in DLAs by adopting Equation 11 and the Al^{III} column density measurements and metallicities reported for $z \sim 2$ (mention pygmy). For sightlines intersecting fewer than 10^{21} hydrogen atoms, we infer $DM_{\text{AIII}} < 30 \text{ pc cm}^{-3}$. The positive correlation between DM_{AIII} and N_{HI} implies that a significant fraction of the observed Al III absorption arises in neutral gas and, therefore, that DM_{AIII} likely overestimates the true contribution to DM from any WIM component.

their complete derivation here but present key expressions, treating angular and temporal broadening separately.

3.1 Angular Broadening

The angular broadening of an image by a point source has radius (half-width at half-maximum),

$$\theta_{\text{scatt}} = f \frac{D_{LS}}{D_S k r_{\text{diff}}} \quad , \quad (12)$$

with f a factor of order unity, D_{LS} and D_S the angular diameter distances from the source to the phase plane and to the source respectively, $k \equiv 2\pi/\lambda_0$ with λ_0 the wavelength in the observer frame, and r_{diff} parameterizes the phase structure function in the form,

$$D_\phi(r) = \left(\frac{r}{r_{\text{diff}}} \right)^{\beta-2} \quad , \quad (13)$$

under the assumption of a power-law spectrum of density inhomogeneities. M13 provide expressions for r_{diff} (see their Equation 7a) in two regimes: (i) $r_{\text{diff}} < \ell_0$, with ℓ_0 the inner scale of the inhomogeneities and; (ii) $r_{\text{diff}} \gg \ell_0$. In the following⁷, we take $\ell_0 = 1 \text{ AU}$ and adopt a Kolmogorov spectrum with $\beta = 11/3$.

⁷ The software accompanying this paper allows for alternate choices for ℓ_0 and β .

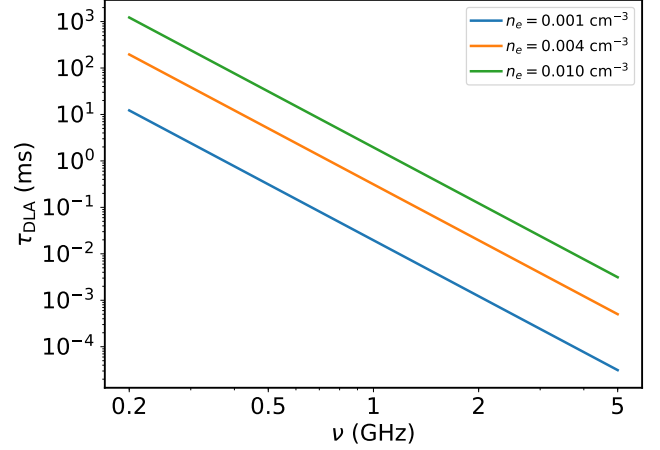


Figure 7. Estimates of the temporal broadening of an FRB by a single, fiducial DLA τ_{DLA} as a function of observed frequency. The DLA has $l_0 = 1 \text{ AU}$, $\Delta L = 1 \text{ kpc}$, $L_0 = 0.001 \text{ pc}$, $z_{\text{DLA}} = 1$, and the source is assumed to be at $z_{\text{FRB}} = 2$. The figure shows values for electron densities spanning best estimations (Neeleman et al. 2015).

In the M13 formalism, r_{diff} is a function of the Scattering Measure (SM) which is an integral over the squared amplitude of density fluctuations along the sightline, $C_N^2(s)$. For extragalactic calculations, one typically introduces an effective Scattering Measure:

$$SM_{\text{eff}} = \int \frac{C_N^2(s)}{(1+z')^2} ds \quad (14)$$

Following Equation 29 of M13, we estimate

$$SM_{\text{eff}} \approx 5.6 \times 10^{16} \text{ m}^{-17/3} \left(\frac{n_e}{10^{-2} \text{ cm}^{-3}} \right)^2 \left(\frac{L_0}{10^{-3} \text{ pc}} \right)^{-2/3} \left(\frac{\Delta L}{1 \text{ kpc}} \right) \left(\frac{2}{1+z_{\text{DLA}}} \right) \quad (15)$$

with ΔL our adopted ‘size’ for a DLA. With the SM_{eff} given above, we estimate $r_{\text{diff}} = 2.2 \times 10^8 \text{ m}$ for $\lambda_0 = 30 \text{ cm}$. This implies an essentially negligible angular broadening of $\approx 0.02 \text{ mas}$ for any source far behind the DLA. We conclude that the ISM of galaxies intervening FRBs will insignificantly broaden the angular size of any background source.

3.2 Temporal Broadening

The other significant effect from turbulent scattering is that multi-path propagation through the medium leads to temporal broadening of the burst. This effect may yield an FRB with much longer observed duration than the intrinsic event and even preclude detection by current and planned experiments (e.g. Chawla et al. 2017).

Following M13, the temporal smearing may be related to angular scattering,

$$\tau_{\text{scatt}} = \frac{D_L D_S \theta_{\text{scatt}}^2}{c D_{LS} (1+z_L)} \quad , \quad (16)$$

The θ_{scatt}^2 term gives a very steep frequency dependence, i.e.

$\tau_{\text{scatt}} \propto \nu^{-\gamma}$ with $\gamma \approx 4-5$, and has an electron density dependence of $\tau_{\text{scatt}} \propto n_e^2$. This is illustrated in Figure 7 for a fiducial DLA with electron densities ranging about our adopted, characteristic value. For $n_e < 10^{-3} \text{ cm}^{-3}$, $\tau_{\text{DLA}} < 1 \text{ ms}$ even for $\nu = 400 \text{ MHz}$ and the effects on the FRB population are likely negligible. Larger n_e values, however, may have observational consequences. For $n_e = 10^{-2} \text{ cm}^{-3}$ and $\nu = 1 \text{ GHz}$, τ_{scatt} exceeds several ms which is comparable to the median width for the current set of observed FRBs (Petroff et al. 2016). Events with $\tau_{\text{scatt}} \gg 5 \text{ ms}$ will have reduced signal-to-noise ($S/N \propto \tau_{\text{scatt}}^{-1/2}$) and those exceeding 100 ms will not trigger most, current FRB search algorithms.

We further emphasize that τ_{scatt} has an explicit $(1+z)^{-1}$ dependence and θ_{scatt} has the same factor implying $\tau_{\text{scatt}} \propto (1+z)^{-3}$. Given the incidence for DLAs remains small for $z_L < 1$, their impact on broadening of the FRB signal is small. From our analysis, we may estimate the fraction of FRB sightlines originating at redshift z_{FRB} that will be broadened by at least τ_{min} . We performed a Monte Carlo simulation of 10^7 sightlines for a series of z_{FRB} values, randomly inserting DLAs from a Poisson distribution with mean $\bar{n}_{\text{DLA}}(z_{\text{FRB}})$. Each DLA is then assigned a random N_{HI} value drawn from $h(N_{\text{HI}})$ to estimate $\Delta L = N_{\text{HI}}/n_{\text{HI}}$ with $n_{\text{HI}} = 0.1 \text{ cm}^{-3}$, and a random electron density. For the latter, we have assumed a Gaussian distribution in $\log n_e$ centered on $\log(n_e/\text{cm}^{-3}) = -2.6$ with a $(0.5 \text{ dex})^2$ variance. For sightlines with multiple DLAs, we add τ_{scatt} in quadrature.

Figure 8 shows the results for several observed frequencies and τ_{min} values. Experiments with $\nu = 1 \text{ GHz}$ are predicted to have only $\approx 0.1\%$ of their sightlines broadened beyond 5 ms. We conclude that the ISM of intervening galaxies has negligible impact on any experiment with $\nu > 1 \text{ GHz}$ (e.g. REALFAST). For $\nu = 600 \text{ MHz}$ (e.g. CHIME), the effects are modest but potentially impactful. Approximately 1% of the sightlines for FRBs at $z_{\text{FRB}} > 1$ are broadened by greater than 5 ms and $\approx 10^{-3}$ have $\tau_{\text{DLA}} > 100 \text{ ms}$. This implies a small but not entirely negligible impact on the population of FRBs discovered at low frequencies. Experiments at even lower frequencies (e.g. LOFAR) will be affected, if the ISM is as modeled here. One can, of course, invert the situation and place constraints on ISM properties by surveying FRBs at a range of frequency.

4 CONCLUDING REMARKS

In this manuscript, we have utilized surveys of DLAs to infer the astrophysical impacts of the ISM in intervening galaxies on FRB events. The principal conclusion is that intervening galaxies will contribute minimally to the integrated DM of an FRB. For a DLA at redshift z_{DLA} , the average contribution from its neutral ISM is $\text{DM}_{\text{DLA}}^{\text{NM}} = 0.25 \text{ pc cm}^{-3} (1+z_{\text{DLA}})^{-1}$ as estimated from the HI column density and n_e/n_{H} distribution functions. Given the low incidence of intervening galaxies, the average contribution along the sightline to an FRB is less than $10^{-1} \text{ pc cm}^{-3}$. From $N(\text{Al}^{++})$ measurements in DLAs, we estimate that the warm ionized component within these galaxies typically contributes $\text{DM}_{\text{DLA}}^{\text{WIM}} < 20 \text{ pc cm}^{-3}$. Similarly, the angular and temporal broadening of FRBs by the ISM of intervening galaxies is nearly negligible for all but the lowest frequency experiments.

While our results indicate that FRB analysis will typi-

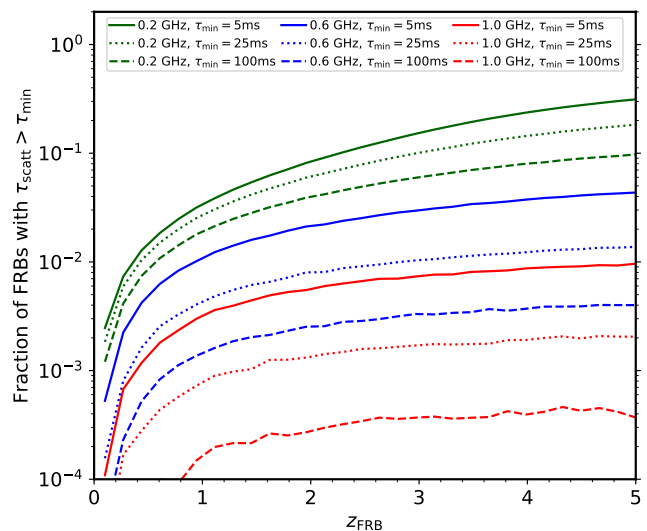


Figure 8. Fraction of sightlines for a population of FRBs at z_{FRB} predicted to experience $\tau_{\text{scatt}} > \tau_{\text{min}}$ for several assumed frequencies. The results are derived from a Monte Carlo simulation with random placement of the redshifts, N_{HI} values, and electron densities [see the text for further details]. Even with $\nu = 600 \text{ MHz}$, the fraction of sightlines that are broadened beyond 25 ms is only approximately 0.1%. We conclude that intersecting galaxies will have a nearly negligible influence on the observed distribution of FRBs.

cally not be sensitive to the ISM of galaxies, there are a few notable exceptions. With a large enough sample across the sky, one may probe the ISM of our nearest neighbors – M31 and the Magellanic Clouds – which span many hundreds of square degrees. Even without precise FRB localizations, one may attribute excess DM and/or temporal smearing from these galaxies.

It is also possible that FRBs frequently occur within the ISM of distant, host galaxies and perhaps within regions of recent/ongoing star-formation. One has gained insight into the properties of such environments from spectroscopy of long-duration gamma ray burst afterglows (e.g. Prochaska et al. 2006; Fynbo et al. 2009). These data reveal highly elevated column densities of neutral hydrogen and associated metals but less evidence for large column densities of ionized gas. There are, however, notable examples of highly saturated high-ion transitions (e.g. Si IV, C IV Mirabal et al. 2003) that indicate large electron column densities and correspondingly large DM values. By assessing the DM contribution to FRBs from gas within their host environments, one will gain new insight into the ISM of distant galaxies.

Throughout this manuscript, we have carefully distinguished between gas within intervening galaxies (i.e. the ISM) from gas surrounding such galaxies (a.k.a. halo gas or the CGM). The latter exhibits a much larger cross-section to absorption and is likely the dominant baryonic component of galaxies (e.g. Werk et al. 2014). In a companion manuscript (Prochaska & Zheng 2017, in prep.), we consider the astrophysical impacts of halo gas on FRBs as inferred from surveys of our Galaxy and the CGM of distant galaxies in absorption.

ACKNOWLEDGEMENTS

We acknowledge valuable input from scientists C. Law, J. Lazio, K. Bannister, and S. Tendulkar.

REFERENCES

- Asplund M., Grevesse N., Sauval A. J., Scott P., 2009, *ARA&A*, **47**, 481
- Bandura K., et al., 2014, in *Ground-based and Airborne Telescopes V*. p. 914522 ([arXiv:1406.2288](#)), [doi:10.1117/12.2054950](#)
- Bannister K. W., et al., 2017, *ApJ*, **841**, L12
- Berkhuijsen E. M., Fletcher A., 2008, *MNRAS*, **390**, L19
- Bird S., Garnett R., Ho S., 2017, *MNRAS*, **466**, 2111
- Bower G. C., et al., 2016, in *American Astronomical Society Meeting Abstracts*. p. 423.09
- Braun R., 2012, *ApJ*, **749**, 87
- Chatterjee S., et al., 2017, *Nature*, **541**, 58
- Chawla P., et al., 2017, preprint, ([arXiv:1701.07457](#))
- Chen H.-W., Prochaska J. X., Weiner B. J., Mulchaey J. S., Williger G. M., 2005, *ApJ*, **629**, L25
- Cordes J. M., Lazio T. J. W., 2003, *ArXiv Astrophysics e-prints*, Crichton N. H. M., et al., 2015, *MNRAS*, **452**, 217
- Davé R., Tripp T. M., 2001, *ApJ*, **553**, 528
- Fall S. M., Pei Y. C., 1993, *ApJ*, **402**, 479
- Fox A. J., Petitjean P., Ledoux C., Srianand R., 2007, *A&A*, **465**, 171
- Fumagalli M., Prochaska J. X., Kasen D., Dekel A., Ceverino D., Primack J. R., 2011, *MNRAS*, **418**, 1796
- Fynbo J. P. U., et al., 2009, *ApJS*, **185**, 526
- Gaensler B. M., Madsen G. J., Chatterjee S., Mao S. A., 2008, *Publ. Astron. Soc. Australia*, **25**, 184
- Hafen Z., et al., 2016, preprint, ([arXiv:1608.05712](#))
- Haffner L. M., et al., 2009, *Reviews of Modern Physics*, **81**, 969
- Howk J. C., Sembach K. R., 1999, *ApJ*, **523**, L141
- Howk J. C., Wolfe A. M., Prochaska J. X., 2005, *ApJ*, **622**, L81
- Inoue S., 2004, *MNRAS*, **348**, 999
- Inoue A. K., Shimizu I., Iwata I., Tanaka M., 2014, *MNRAS*, **442**, 1805
- Kanekar N., Chengalur J. N., 2003, *A&A*, **399**, 857
- Kanekar N., et al., 2014, *MNRAS*, **438**, 2131
- López S., et al., 2016, *A&A*, **594**, A91
- Macquart J.-P., Koay J. Y., 2013, *ApJ*, **776**, 125
- Maller A. H., Prochaska J. X., Somerville R. S., Primack J. R., 2003, *MNRAS*, **343**, 268
- McQuinn M., 2014, *ApJ*, **780**, L33
- Mirabal N., et al., 2003, *ApJ*, **595**, 935
- Neeleman M., Wolfe A. M., Prochaska J. X., Rafelski M., 2013, *ApJ*, **769**, 54
- Neeleman M., Prochaska J. X., Wolfe A. M., 2015, *ApJ*, **800**, 7
- Neeleman M., Prochaska J. X., Ribaldo J., Lehner N., Howk J. C., Rafelski M., Kanekar N., 2016, *ApJ*, **818**, 113
- Noterdaeme P., Petitjean P., Ledoux C., Srianand R., 2009, *A&A*, **505**, 1087
- Noterdaeme P., et al., 2012, *A&A*, **547**, L1
- Ostriker J. P., Heisler J., 1984, *ApJ*, **278**, 1
- Parks D., Prochaska J. X., Dong S., Cai Z., 2017, preprint, ([arXiv:1709.04962](#))
- Petroff E., et al., 2016, *Publ. Astron. Soc. Australia*, **33**, e045
- Planck Collaboration et al., 2016, *A&A*, **594**, A13
- Prochaska J. X., Wolfe A. M., 2009, *ApJ*, **696**, 1543
- Prochaska J. X., Howk J. C., O'Meara J. M., Tytler D., Wolfe A. M., Kirkman D., Lubin D., Suzuki N., 2002, *ApJ*, **571**, 693
- Prochaska J. X., Herbert-Fort S., Wolfe A. M., 2005, *ApJ*, **635**, 123
- Prochaska J. X., Chen H.-W., Bloom J. S., 2006, *ApJ*, **648**, 95
- Prochaska J. X., Chen H.-W., Wolfe A. M., Dessauges-Zavadsky M., Bloom J. S., 2008a, *ApJ*, **672**, 59
- Prochaska J. X., Hennawi J. F., Herbert-Fort S., 2008b, *ApJ*, **675**, 1002
- Rand R. J., 1997, *ApJ*, **474**, 129
- Rao S. M., Turnshek D. A., Nestor D. B., 2006, *ApJ*, **636**, 610
- Rao S. M., Turnshek D. A., Sardane G. M., Monier E. M., 2017, preprint, ([arXiv:1704.01634](#))
- Reynolds R. J., Tufte S. L., Haffner L. M., Jaehnig K., Percival J. W., 1998, *Publications of the Astronomical Society of Australia*, **15**, 14
- Ribaldo J., Lehner N., Howk J. C., 2011, *ApJ*, **736**, 42
- Sánchez-Ramírez R., et al., 2016, *MNRAS*, **456**, 4488
- Savage B. D., Edgar R. J., Diplas A., 1990, *ApJ*, **361**, 107
- Sofia U. J., Jenkins E. B., 1998, *ApJ*, **499**, 951
- Spitler L. G., et al., 2016, *Nature*, **531**, 202
- Storrie-Lombardi L. J., Wolfe A. M., 2000, *ApJ*, **543**, 552
- Taylor J. H., Cordes J. M., 1993, *ApJ*, **411**, 674
- Tejos N., et al., 2014, *MNRAS*, **437**, 2017
- Tendulkar S. P., et al., 2017, *ApJ*, **834**, L7
- Viegas S. M., 1995, *MNRAS*, **276**, 268
- Vladilo G., Centurión M., Bonifacio P., Howk J. C., 2001, *ApJ*, **557**, 1007
- Werk J. K., et al., 2014, *ApJ*, **792**, 8
- Wolfe A. M., Prochaska J. X., 2000a, *ApJ*, **545**, 591
- Wolfe A. M., Prochaska J. X., 2000b, *ApJ*, **545**, 603
- Wolfe A. M., Turnshek D. A., Smith H. E., Cohen R. D., 1986, *ApJS*, **61**, 249
- Wolfe A. M., Lanzetta K. M., Foltz C. B., Chaffee F. H., 1995, *ApJ*, **454**, 698
- Wolfe A. M., Prochaska J. X., Gawiser E., 2003, *ApJ*, **593**, 215
- Wolfe A. M., Gawiser E., Prochaska J. X., 2005, *ARA&A*, **43**, 861
- Wolfire M. G., Hollenbach D., McKee C. F., Tielens A. G. G. M., Bakes E. L. O., 1995, *ApJ*, **443**, 152
- Worseck G., Prochaska J. X., 2011, *ApJ*, **728**, 23
- Worseck G., et al., 2014, *MNRAS*, **445**, 1745
- Zwaan M. A., Meyer M. J., Staveley-Smith L., Webster R. L., 2005, *MNRAS*, **359**, L30

This paper has been typeset from a $\text{\TeX}/\text{\LaTeX}$ file prepared by the author.

Table 1. N_{HI} MEASUREMENTS

Measure	Param.	Unit	Value	16th	84th	0.5th	99.5th
$h(N_{\text{HI}})$	N_d		21.551				
	α_3		-2.055				
	α_4		-6.000				
$\ell_{\text{DLA}}(z)$	A		0.236	0.214	0.255	0.186	0.305
	B		0.168	0.150	0.177	0.132	0.214
	C		2.869	2.717	3.020	2.465	3.323
DM_{DLA}^a		pc cm^{-3}	0.18	0.5 dex	0.5 dex	1.0 dex	1.0 dex
$\overline{DM}_{\text{DLA}}^{\text{NM}}(z_{\text{FRB}} = 1)$		pc cm^{-3}	0.004	0.000	0.000	0.000	0.183
$\overline{DM}_{\text{DLA}}^{\text{NM}}(z_{\text{FRB}} = 2)$		pc cm^{-3}	0.010	0.000	0.000	0.000	0.218
τ_{DLA}^b		ms	0.31				

^aRest-frame value. Error is dominated by uncertainty in n_e .

^bAssumes $\nu = 1\text{GHz}$, $n_e = 4 \times 10^{-3} \text{cm}^{-3}$, $z_{\text{DLA}} = 1$, $z_{\text{source}} = 2$.